Chapter 1

Introduction

1.1 Overview of Vacuum Microelectronics

1.1.1 History of Vacuum Microelectronics

When the first semiconductor transistor was invented by Bardeen, Brattain, and Shockley in the 1950s[1.1], and integrated circuits were subsequently developed in the 1960s[1.2], people generally thought that the time of using vacuum tubes was over. Gradually, vacuum tubes were replaced by solid state electronic devices due to their tiny volume, low cost, better reliability, and high power efficiency. For the past decades, great improvements on semiconductor manufacturing technology gave a new life to vacuum electronics for the professional micro fabrication process to fabricate tiny vacuum devices, which is now called vacuum microelectronics. “Vacuum state” devices have a great deal of superior advantages as compared with solid-state devices, including fast carrier drift velocity, radiation hardness, and temperature insensitivity. For example, the saturation drift velocity is limited to less than 3×10^{7} cm/s in all semiconductor due to scattering mechanism whereas the saturation drift velocity in vacuum is limited theoretically to 3×10^{10} cm/s and practically to about 6-9$\times10^{8}$ cm/s [1.3]. Furthermore, temporary or permanent radiation effect is negligible in vacuum devices for no medium being damaged. Additionally, the effect of temperature on performance is reduced in vacuum devices simply for no medium causing the temperature effect in semiconductor, such as increased lattice scattering or bulk carrier generation/recombination. Table 1-1 shows the comparison between vacuum microelectronic

and semiconductor devices.

In order to accomplish better understanding of the advantages of vacuum microelectronics, a brief history of the field emission theory and vacuum microelectronic devices is necessary. Recent developments in vacuum microelectronics started in 1928, when R. H. Fowler and L. W. Nordheim published the first theory of electron field emission from metals using quantum mechanics [1.4]. This theory is different from thermionic emission, which metal has to be heated so that some of the electrons in the metal gain enough thermal energy to overcome the metal/vacuum barrier; according to the Fowler-Nordheim theory, an applied electric field of approximately 10^3 V/μm is needed for electrons to tunnel through the sufficiently narrow barrier [1.4]. To reach this high field at reasonable applied voltage, producing the field emitters into protruding objects is essential to take advantage of field enhancement. It was not until 1968 when C. A. Spindt camp up with a fabrication method to create very small dimension metal cones that vacuum microelectronic triodes became possible [1.5]. From the late 1960s to the year 1990, Ivor Brodie, Henry F. Gray, and C. A. Spindt made many contributions in this field. Also, most of research was focused on the devices similar to the Spindt cathode during the past three decades.

In 1991, a group of research of the French company LETI CHEN reported a microtip display at the fourth International Vacuum Microelectronics Conference [1.6]. Their display was the first announcement of a practical vacuum microelectronic device. From then on, a great amount of researchers all over the world are devoted themselves to this interesting, challenging, and inventive field. Part of the work focused on fabricating very small radius silicon tip by utilizing modern VLSI technology [1.7-1.8]. Some of them increased the emission current by coating different metals, such as W, Mo, Ta, Pt etc., even diamond on field emission arrays [1.9-1.11]. Different device schemes also have been proposed to enhance the emission current density, stability, and reliability.

1.1.2 Application of Vacuum Microelectronics

Due to the superior properties of vacuum microelectronic devices, potential applications include high brightness flat-panel display [1.12-1.16], high efficiency microwave amplifier and generator [1.17-1.19], ultra-fast computer, intense electron/ion sources [1.20-1.21], scanning electron microscopy, electron beam lithography, micro-sensor [1.22-1.23], temperature insensitive electronics, and radiation hardness analog and digital circuits.

Among wide range applications of the vacuum microelectronics, the first commercial product could be the field emission flat-panel display. The field emission fluorescent display is basically a thin cathode ray tube (CRT), which was first proposed by SRI International and later demonstrated by LETI [1.6].

Various kinds of flat-panel displays, such as liquid crystal display (LCD), electroluminescent display (EL), vacuum fluorescent display (VFD), plasma display panel (PDP), and light emitting display (LED), are developed for the better characteristics of small volume, light weight, and low power consumption. LCDs have become the most popular flat panel displays, however, LCDs have some drawbacks, such as poor viewing angle, temperature sensitivity and low brightness. As a result, some opportunities still exist and waiting for the solutions from other flat panel displays such as FED.

FED features all the pros of the CRTs in image quality and is flat and small volume. The schematic comparisons are revealed in Fig.1-1. The operation of CRTs involves deflection of the beam in such a way that the electron spot scans the screen line-by-line. In FEDs, multiple electron beams are generated from the field emission cathode and no scanning of beams is required. The cathode is a part of the panel substrate consists of an X-Y electrically addressable matrix of field emission arrays (FEAs). Each FEA is located at the intersection of a row and a column conductor, with the row conductor serving as the gate electrode and the

column conductor as the emitter base. The locations where the rows and columns intersect define a pixel. The pixel area and number of tips are determined by the desired resolution and luminance of the display. Typically, each pixel contains an FEA of 4-5000 tips. The emission current required for a pixel varies from 0.1 to 10 μA, depending on the factors such as the luminance of the display, phosphor efficiency and the anode voltage.

Compared to the active matrix LCDs, FEDs generate three times the brightness with wilder viewing angle at the same power level. Full color FEDs have been developed by various research groups from different aspects such as PixTech, Futaba, Fujitsu, Samsung, are presently engaged in commercially exploiting FED.

Either vacuum or solid-state devices can generate power at frequency in the GHz range. Solid-state devices, such as impact avalanche transit time (IMPATT) diodes, Si bipolar transistors, and GaAs FETs [1.24], are typically used in the lower power (up to 10 W) and frequency (up to 10 GHz) range. Vacuum devices still remain the only technology available for high power and high frequency applications. These devices include traditional multi-terminal vacuum tubes, like triodes, pentodes, and beam power tubes, and distributed-interaction devices, such as traveling wave tubes (TWTs), klystrons, backward-wave oscillators (BWOs).

The performance of FEAs in conventionally modulated power tubes, like TWT, is determined primarily by their emission current and current density capability. On the other hand, the application of FEAs in the microwave tubes in which modulation of the beam is accomplished via modulation of the emission current at source, such as capacitance and transconductance. Successful operation of a gated FEA in a 10 GHz TWT amplifier with conventional modulation of electron beam has been demonstrated by NEC Corporation of Japan [1.25]. The amplifier employed a modified Spindt-type Mo cathode with circular emission area of 840 μm in diameter. The modified cathode structure incorporated a resistive

poly-Si layer as a current limiting element. The emission current from the cathode was 58.6 mA. The prototype TWT could operate at 10.5 GHz with the output power of 27.5 W and the gain of 19.5 dB. The bandwidth of the tube was greater than 3 GHz. The prototype was operated for 250 h.

1.2 Novel Nano-sized Materials for Field Emission Display

1.2.1 Theory Background

Electron field emission is a quantum mechanical tunneling phenomenon of electrons extracted from the conductive solid surface, such as a metal or a semiconductor, where the surface electric field is extremely high. If a sufficient electric field is applied on the emitter surface, electrons will be emitting through the surface potential barrier into vacuum, even under a very low temperature. In contrast, thermionic emission is the hot electron emission under high temperature and low electric field. Fig. 1-2(a) demonstrates the band diagram of a metal-vacuum system.

Here W_0 is the energy difference between an electron at rest outside the metal and an electron at rest inside the metal, whereas W_f is the energy difference between the Fermi level and the bottom of the conduction band. The work function ϕ is defined as $\phi = W_0 - W_f$. If an external bias is applied, vacuum energy level is reduced and the potential barrier at the surface becomes thinner as shown in Fig. 1-2(b). Then, an electron having energy "W" has a finite probability of tunneling through the surface barrier. Fowler and Nordheim derive the famous F-N equation (1.1) as follow [1.4]:

$$J = \frac{AE^2}{\phi t^2(y)} \exp[-B\phi^{\frac{3}{2}} v(y)/E], \tag{1-1}$$

where J is the current density (A/cm^2). E is the applied electric field (V/cm), ϕ is the work function (in eV), A = 1.56×10^{-6}, B = -6.831×10^{-7}, y = 3.79x10^{-4}×10^{-4}E$^{1/2}$/ϕ, t^2(y)~1.1 and v(y) can be approximated as [1.26]

$$v(y) = \cos(0.5\pi y), \tag{1-2}$$

or

$$v(y) = 0.95 - y^2. \tag{1-3}$$

Typically, the field emission current I is measured as a function of the applied voltage V. Substituting relationships of J = I/α and E = βV into Eq.(1-1), where α is the emitting area and β is the local field enhancement factor of the emitting surface, the following equation can be obtained

$$I = \frac{A\alpha\beta^2 V^2}{\phi t^2(y)} \exp[-Bv(y)\frac{\phi^{\frac{3}{2}}}{\beta V}]. \tag{1-4}$$

Then taking the log. form of Eq. (1-4) and v(y) ~ 1

$$\log(\frac{I}{V^2}) = \log[1.54\times10^{-6}\frac{\alpha\beta^2}{\phi t^2(y)}] - 2.97\times10^7(\frac{\phi^{3/2}v(y)}{\beta V}), \tag{1-5}$$

from Eq. (1-5), the slope of a Fowler-Nordheim (F-N) plot is given by

$$S \equiv slope_{FN} = -2.97\times10^7(\frac{\phi^{\frac{3}{2}}}{\beta}), \tag{1-6}$$

The parameter β can be evaluated from the slope S of the measured F-N plot if the work function ϕ was known

$$\beta = -2.97\times10^7(\frac{\phi^{\frac{3}{2}}}{S}) \ \ (\text{cm}^{-1}), \tag{1-7}$$

The emission area α can be subsequently extracted from a rearrangement of Eq. (1-5)

$$\alpha = (\frac{I}{V^2})\frac{\phi}{1.4\times10^{-6}\beta^2}\exp(\frac{-9.89}{\sqrt{\phi}})\exp(\frac{6.53\times10^7\phi^{\frac{3}{2}}}{\beta V}) \quad (\text{cm}^2). \tag{1-8}$$

For example, the electric field at the surface of a spherical emitter of radius r concentric with a spherical anode (or gate) of radius r+d can be represented analytically by

$$E = \frac{V}{r}(\frac{r+d}{d}), \tag{1-9}$$

Though a realistic electric field in the emitter tip is more complicated than above equation, we can multiply Eq.(1-9) by a geometric factor $\beta`$ to approximate the real condition.

$$E_{tip} \equiv \text{function of (r,d)} = \beta`\frac{V}{r}(\frac{r+d}{d}), \tag{1-10}$$

where r is the tip radius of emitter tip, d is the emitter-anode(gate) distance and $\beta`$ is a geometric correction factor [1.27].

For a very sharp conical tip emitter, where d >> r, E_{tip} approaches to $\beta`$(V/r). And for r>>d, $E_{tip}$ approaches to $\beta`$(V/d) which is the solution for a parallel-plate capacitor and for a diode operation in a small anode-to-cathode spacing. As the gated FEA with very sharp tip radius, Eq. (1-10) can be approximated as:

$$E_{tip} = \beta`(\text{V/r}). \tag{1-11}$$

Combining E= βV and Eq. (1-11), we can obtain the relationship:

$$E_{tip} = \beta\text{V} = \beta`(\text{V/r}), \text{ and } \beta` = \beta\text{r}. \tag{1-12}$$

The tip radius r is usually in the range from a few nm to 50 nm, corresponding to the parameter $\beta`$ ranging from 10^{-1} to 10^{-2}.

Besides, transconductance g_m of a field emission device is defined as the change in anode

current due to a change in gate voltage [1.3].

$$g_m = \frac{\partial I_C}{\partial V_g}|_{Vc} \ , \tag{1-13}$$

Transconductance of a FED is a figure of merit that gives as an indication of the amount of current charge that can be accomplished by a given change in grid voltage. The transconductance can be increased by using multiple tips or decreasing the cathode-to gate spacing for a given cathode-to-anode spacing.

According to the equations above mentioned (especially Eq.1-5), the following approaches may therefore be taken to reduce the operating voltage of the field emission devices:

（1） Find techniques to reproducibly sharpen the tips to the atomic level (increase β).

（2） Lower the work function of the tip (ϕ)

（3） Narrow the cone angle (increase β).

（4） Reduce the gate-opening diameter (increase β).

1.2.2 Cold Cathode Structures and Materials for Field Emission Display

FED is one of the most promising emissive type flat-panel display, which can overcome the drawbacks of TFT-LCD. However, some difficult technological subjects should be considered such as microfabrication of cathodes, assembly technology with accuracy of micrometer level, packaging of vacuum panel with thin-glass substrates, vacuum technology to keep stable field emission in small space of flat panels, selection of suitable materials to keep a high vacuum condition in panels and high efficiency phosphor materials. The researching objects of this thesis are to produce novel cathode structure and synthesis of novel

emitter materials for FED operations. The experimental background is introduced in the following paragraphs.

A. Spindt-type field emitters

Figure 1-3 demonstrated the scanning electron microscope (SEM) and schematic images of a spindt type field emission triode [1.28], which was invented by Spindt of SRI and improved for the electron source of high-speed switching devices or microwave devices [1.29]. Meyer of LETI presented the capability of using Spindt-type emitters for a display in 1970s [1.30] and stabilized the field emission from Spindt-type emitters by introducing a resistive layer as the feedback resistance. This proposal triggered the development of field emitters as an electron source of displays by researchers and electronics makers in 1990. The merits of the Spindt type field emitters are summarized as following: (1) High emission current efficiency, more than 98% anode current to cathode current can be achieved for the symmetric structure of Spindt tip and the gate hole, the lateral electric field to the metal tip can be cancelled out. (2) The fabrication is self-aligned, easy process; uniform field emission arrays can be fabricated easily. Some research groups have successfully fabricated commercial FED products based on Spindt type field emitters such as Futaba, Sony/Candesent, Futaba and Pixtech.[1.31], the products above mentioned companies are shown in Figures 1-4.

However, there are some existing drawbacks of Spindt type field emitters when fabricating Spindt type FED such as (1) High gate driving voltage required; for a Spindt type field emission triode with 4 μm gate aperture, the driving voltage is typically more than 60 V, which results in the high cost of the driving circuits. To reduce the gate driving voltage, frontier lithography technologies such as E beam lithography must be applied to reduce the gate aperture to the sub-micron level. (2) The emission property degrades for the chemically instable of the metal tips. (3) Huge, expensive high vacuum deposition system required during

fabricating large area Spindt type FED.

B. Si tip field emitters

An alternative approach to fabricate tip type field emitters is to fabricate the Si tip field emitters based on the semiconductor fabricating process. Figures 1-5(a) and (b) depict the SEM micrographs of Si tips array and Si tip field emission triodes array formed by chemical mechanical polishing (CMP) [1.32] Symmetric device structure and similar advantages with Spindt type field emitters can be obtained, However, high temperature oxidation sharpening process prohibits Si tip from large area fabrication.

C. Carbon and Nano-sized Emitters

Carbon nanotubes have attracted a great deal of interests owing to their advantageous properties, such as high aspect ratios, small tip radius of curvature, high Young's modulus, capability for the storage of a large amount of hydrogen, and structural diversities that make it possible for band gap engineering. These useful properties of carbon nanotubes (CNTs) make themselves good candidates for various applications, for instance, wires for nanosized electronic devices, super strong cables, AFM tips, charge-storage devices in battery, and field emission display.

According to Fowler-Nodheim theory, the electric field at the apex of a needle-shaped tip is enhanced by a factor $\beta = h/r$, where h is the height of the tip and r is the radius of curvature of the tip apex. The carbon nanotube is a stable form of carbon and can be synthesized by several techniques. They are typically made as threads about 10-100 nm in diameter with a high aspect ratio (>1000). These geometric properties, coupled with their high mechanical strength and chemical stability, make carbon nanotubes attractive as electron field emitters. Several groups have recently reported good electron field emission from nanotubes [1.33-1.35].

In 1999, Samsung pronounced a 4.5-inch carbon nanotube based field emission display. They mixed a conglomeration of single-walled CNTs into a paste with a nitrocellulose binder and squeezed the concoction through a 20-μm mesh onto a series of metal strips mounted on a glass plate. As the CNTs emerged from the mesh, they were forced into a vertical position. The metal strips with the CNTs sticking out of them served as the back of the display. The front of the display was a glass plate containing red, green, and blue phosphors and strips of a transparent indium-tin-oxide anode running from side to side. The glass plates were separated by spacers with the thickness of 200 μm. Once assembled, the edges were sealed and air was pumped out of the display.

Samsung's field emission display (Fig. 1-6) could be the precursor of a new generation of more energy efficient, high performance flat panel displays for portable computers [1.36]. The CNTs appear to be durable enough to provide the 10000hr lifetime considered being a minimum for an electronic product. The panel consumes just half the power of an LCD to generate an equivalent level of screen brightness. They could also be cheaper than LCDs or other types of field emission displays being developed. Until now, at last five major Japanese electronic manufactures are working on this technology.

1.3 A Great Discovery of Nano Electronic Technology—Carbon Nanotubes

1.3.1 Structures of Carbon Nanotubes

Carbon nanotubes are cylindrical molecules consisting of single or multi-graphite layers. Unlike other covalent matters, carbon shows various structures. The common allotropes of carbon are (1) graphite, (2) diamond, and (3) fullerene (Fig. 1-7). Among them, graphite is a

planar structure of carbon in sp^2 bonding. As the scale of graphite is close to the nano scale, it could curl and form a hollow tube. According to the number of layers in the tube wall, we classify the carbon nanotubes into two kinds: (1) single-walled (SWNTs) and (2) multi-walled carbon nanotubes (MWNTs) (Fig. 1-8).

A. Single-walled Carbon Nanotubes

The curling direction of graphite decides the characteristics of single-walled carbon nanotubes, like metal or semiconductor. Based on the curling direction, we can classify SWNTs into three kinds: (1) armchair, (2) zigzag, (3) chiral. The armchair SWNTs reveal metallic property. The zigzag and chiral SWNTs display both of metallic and semiconductoring properties.

B. Multi-walled Carbon Nanotubes

Since the distance between layers in MWNTs must satisfy 0.34nm, the curl direction of every layer may be different. MWNTs present different morphology by various growing parameters. In terms of appearance, we can approximately categorize MWNTs into several types: (1) standard tube, (2) spiral, (3) "Y" model. If we further investigate the microstructure of the MWNTs, we can observe that there are different structures such as hollow-liked, bamboo-liked and fish-bone-liked MWNTs.

1.3.2 Properties and Synthesis of Carbon Nanotubes

Carbon nanotubes have several superior characteristics, such as high thermal conductivity, good heat resistance, low chemical reactivity, and high aspect ratio [1.37]. These qualities are suitable for a field-emission source. Moreover, due to the combination of their high mechanical strength, light weight and excellent chemical and thermal stability, carbon

nanotubes emerge as a new class of materials with a broad range of potential applications. This is why there are many groups currently studying on CNT synthesis and expanding the purpose of CNTs in the future.

Fe, Co, and Ni particles are known to be the catalyst for vapor grown CNT synthesis in which hydrocarbons and H_2 gases react with the presence of Fe, Co, or Ni particles in a reaction tube. By means of the carbon atoms diffusing and dissolving at the surface of the catalyst nano-particles, the carbon atoms in the catalyst nano-particles achieve saturation and then precipitate to form CNTs (Fig. 1-9 [1.38]). The synthetic procedure of CNTs mentioned above is famous chemical vapor deposition. Other common methods of CNT synthesis include: (1) arc-discharge, (2) laser ablation, (3) solar energy, and (4) microwave plasma enhanced chemical vapor deposition.

1.3.3 Potential Application of Carbon Nanotubes

Since the discovery of CNTs in 1991, they have been attracting much attention for their unique physical and chemical properties. Their extensively potential applications lead them to become a super star of nano technology, which cover: (1) Field Emission Display (FED), (2) Field Effect Transistor, (3) Nano-conducting Wire, (4) Vehicles for Hydrogen Storage, (5) Probe of AFM and etc. [1.39].

In the wide-ranging applications of CNTs, FED arouses researchers' interest particularly. In virtue of the superior field emission characteristics, CNTs are applied to the emitting source of cold cathode. The advantages of FED are its low response time, wide view angle, high brightness, high working temperature range and well combination with mature phosphor technology. However, a major problem needs to be solved in this field. It is not allowed to effectively analyze CNTs on a flat panel at relatively lower temperature (<500°C) and this

barrier restriction obstructs the development of CNT-FED so far.

1.4 Thesis Organization

The overview of vacuum microelectronics and basic principles of field emission theory was described in chapter 1. Moreover, the properties and applications of CNTs were presented clearly.

Several papers about CNTs grown at low temperature for FED application were depicted in chapter 2. Then we referred to the motivation in this chapter.

The experimental procedures were revealed in chapter 3. First, we grew CNTs on Si substrate at low temperature. Then, the improvement of gate controlled anode current was proposed. Finally, CNTs were grown on glass substrate for FED application.

Results and discussion were charactered in chapter 4. And the luminescent image from CNTs on glass substrate obtained on the anode phosphor substrate was the most important result.

Finally, the conclusions and recommendations for future researches are provide in chapter 4.

Chapter 2

Paper Review and Motivation

2.1 Paper Review

2.1.1 Overview of CNTs Grown at Low Temperature

Carbon nanotubes are the most important materials for field emission displays (FED) due to their superior emission characteristics as described in the previous section 1.3.2. Therefore, CNTs are attributed to be one of the most attractive of potential field emitters for flat-panel displays. Considering the direct growth of CNTs on the substrate, thermal CVD is often used since the damage to the substrate is small [2.1]. The reaction temperature of thermal CVD is generally higher than 700℃ in earlier experiments. There are two critical purposes to grow CNTs at higher temperature. One is to gain fine catalyst nanoparticles after pretreatment, and the other is to obtain fine graphite structure of CNTs [2.2-2.4].

Recently, the direct growth of CNTs on glass substrate by thermal CVD at low temperature has been researched for the fabrication of field emission displays. For practical application, soda lime glass is one of the most preferable materials for the cathode substrate of filed emission displays because of its cheapness. Although using soda lime glass substrate indeed costs down, the melting point of 570℃ restricts the processing temperature when growing CNTs by thermal CVD. Some methods are proposed to replace traditional CVD, and one of the best known is “screen printing” [2.5-2.6]. Low cost, high brightness, and simple process are the advantages of the screen printing method, yet CNT distribution by screen printing are non-uniform. Consequently, the resolution of the flat-panel displays by this way is

degraded seriously. Owing to the higher throughput and better uniformity, thermal CVD is still the most attractive method for CNT growth.

In the field of CNT-FED fabrication, how to grow uniform CNT films at low temperature has been one of the most difficult problems. Great efforts have been invested in this topic to fabricate field emission displays on a large area flat-panel. In our group, we used MPCVD to grow CNTs in the past. Changeful range of the plasma resulted in high temperature of the surface of the substrate, and the real temperature during the growth of the CNTs was not sure. Therefore, we attempted to grow CNTs by thermal CVD since last year and successfully grow uniform CNTs on a large area so far.

2.1.2 Theoretical Background

Catalyst plays an important role in growing CNTs by CVD. Two main capabilities of it are: (1) to help with the decomposition of hydrocarbon gas, and (2) to let carbon atom diffuse in the catalyst nano-particles. The composition of the catalyst influences the growth of CNTs greatly. According to the Tammann's rule, the temperature which atoms start moving is called "Tammann temperature". It is about 1/3 of the melting point of metal (T_T=0.3T_m K). Physical properties of some common catalysts are shown in Table 2-1.

Catalyst must be transformed into nano-particles in the pre-treatment stage. In light of Lindemann criterion, the melting point decreases abruptly when the catalyst is close to nano-size (Fig 2-1). After being formed, nanoparticles will help the decomposition of gas source and the diffusion of the carbon atom. Fig. 2-2 shows the role of catalyst in the pretreatment and growth stages. We need such a kind of catalyst with lower melting point and Tammann temperature. As shown in Table 2-1, the melting point of the mono-metal is not low enough for CNTs to grow below 500℃. This may be the reason why many groups focus on

the research in novel catalyst with lower melting point.

The proposition of “low-temperature growth of carbon nanotubes by thermal CVD with FeZrN catalyst” is first held by Shiroishi et al. [2.7]. They compared the FeZrN and Fe film after pre-treatment, later finding the orderly film particles on the surface of the FeZrN rather than on the surface of the Fe film. This means that FeZrN film is more easily changed into fine particles at a low temperature than Fe film. The fine particles are needed as a precursor of CNTs, and CNTs themselves are successfully synthesized at 500-550℃.

Cobalt-containing amorphous carbon composite films were employed as a catalyst layer for the growth of CNTs by decomposing acetylene in a tube furnace [2.8]. Mirror-like smooth carbon nanotube films were grown by thermal CVD on glass substrate at a relatively low temperature of 570℃.

Catalytic layers of an Invar 426 alloy (42%Ni, 52%Fe, and 6%Co) were prepared for CNT growth at low temperature in Park et al.’s study [2.9]. CNTs were grown by thermal decomposition of CO and H_2 gases at atmospheric pressure for different Invar (Fe-Ni-Co alloy) catalytic layers. In this study, they carried out the synthesis of CNTs by thermal CVD on glass substrates at temperature as low as 500-550℃.

At low temperature by a thermal CVD method, Kamada et al. have grown CNFs (carbon nanofiber) successfully on Pd-Se, Fe-Ni, and Ni-Cu alloy catalysts [2.10]. Among these alloy catalysts, Ni-Cu alloy catalysts were found to be the most suitable for low temperature growth of CNF (400℃). By using Pd-Se and Fe-Ni alloy as the catalysts, CNFs were grown at the lowest temperature of 500℃.

In addition to the focus on the catalysts, a new process of thermal CVD is advanced by Cheol et al. [2.11]. They employed a two-stage heating technique with which the reactants heated at 850℃ in the first zone flow into the second zone maintained at 550℃ for CNT

growth. Fig. 2-3 is a schematic diagram showing the two different temperature zones of CVD reactor. The first heating (high temperature) zone was maintained at 850℃ to activate the reactant gas. The temperature of second heating (low temperature) zone was controlled to be 550℃.

In growing CNTs at low temperature, the reactant (gas source) is a critical element as well. Four hydrocarbon gases are studied: C_2H_2 (acetylene) with a C-C triple bond, C_2H_4 (ethylene) with a double bond, C_2H_6 (ethane) with a single bond, and CH_4 (methane). The chemical activation of these compounds is related to their heat of formation, obtained from *CRC Handbook of Physics and Chemistry*, and shown in Fig. 2-4. In general, the greater the bond number is, the more reactive the gases are [2.12].

2.1.3 Improvement of Gated Triode Structure

For improvement of gate controlled anode current, CNT-FED with planar-gate and under-gate structure (Fig. 2-5) was also explored [2.13-2.16]. In the study conducted by Lan et al., how the current density distributed on anode plate and how the display's resolution was affected by the bias conditions of the emitter were investigated. For the planar triode structure, the good resolution is achieved when the gate voltage is adjusted to converge on the electron beams to an anode plate. For the under-gate structure, the display has a good resolution provided that the gate voltage is not too large to pull out the electrons to strike on other pixels. In general, the under-gate structure has a wider gate-biased operating condition, but the planar-gate structure has a higher light efficiency under the same resolution.

In the under-gate structure, gate electrodes are located underneath cathode electrodes with an in-between insulating layer, which is the so-called under-gate triode structure. In the under-gate structure, gate electrodes are under the cathode, on the opposite side of the anode,

in which case it seems for emission electrons hardly to move toward the anode. Recently, Choi et al. fabricated a fully sealed FED panel of 4.5 in. diagonal size with single walled carbon nanotubes [2.17]. They employed a paste squeeze technique, which opened a way to integrate large FED panels based on CNT emitters. However, their work was restricted to a diode structure. For full gray-scale image and fast response for moving pictures, a triode structure is necessary. In this study, we investigated a new triode structure of FEDs with CNT emitters and designated an under-gate triode [2.18] type where gate electrodes are located under cathode electrodes. Although triode-type FEAs are essential for practical FED applications in order to realize low voltage driving, high resolution and full gray-scale imaging, the papers regarding the fabrication of the triode type CNT FEAs have been few.

2.1.4 CNTs Grown on Glass Substrate

Jung et al. developed a photosensitive paste including single walled CNTs for screen printing on glass substrate [2.19]. CNT emitter dots with the diameter of 5 um were defined inside gate holes with a diameter of 10 um by screen printing the CNT paste and a subsequent backside photolithography. Recently, screen printing technology is one of the common methods used for fabrication of FED on glass substrate.

A triode structure with a counter electrode on glass substrate was presented by Uh et al. [2.15]. In their experiment, triode-type field emitter arrays (FEAs) were fabricated successfully by using carbon nanotubes as electron emission sources on glass substrate.

For the filed emission display application, CNTs grown on glass substrate becomes the trend. In order to improve the uniformity of screen printing, there must be an effective process for CNTs grown at low temperature by thermal CVD. CNTs grown on Si and glass substrate show different morphology, so the stability of CNT characteristics, including morphology and

field emission properties on glass substrate, must be controlled.

2.2 Motivation

2.2.1 CNTs Grown at Low Temperature

To commercialize the field emission display, fabrication field emission cathodes with low operation voltage, high emission current, excellent stability and good reliability are crucial. According to the F-N equation, the work function ϕ of the cathode material must be as low as possible and the field enhancement factor β and emission area α should be as large as possible in order to achieve the high emission currents at low applied voltages.

CNTs were also synthesized as the field emitters for the nanosized feature, which can provide large aspect ratio to increase the field enhancement factor β. The high density of the nanotubes also provides the large emission site density (increasing the emission area α). Different kinds of catalyst for CNT growth were investigated in this thesis.

We used FeNi as the catalyst instead of Fe or Ni for CNT growth at low temperature. It was indicated that Ni might promote the stability of γ-Fe, which was beneficial for the diffusion of carbon atom. Therefore, it was inferred that FeNi catalyst was more suitable than Fe or Ni in growing CNTs, especially at low temperature. From our experimental results, we found that FeNi alloy was obviously not effective for CNT growth at low temperature. We believed that it should be confined by the Tammann's temperature. The hypothesis then came to be proven soon by the phase diagram as shown in Fig. 2-6 [2.13], exhibiting that the eutectic point of FeNi alloy seems to be almost the same as the melting point of Fe or Ni.

According to the Lindemann criterion and Tammann's rule, NiPd and FeC are essential to be brought out for CNT growth at low temperature. Fig. 2-7 (a) and (b) are the phase

diagrams of NiPd and FeC respectively [2.20]. It is manifest that the eutectic point of NiPd or FeC is lower than FeNi. This is why we chose them to grow CNTs at low temperature (500℃). In the thesis, the successful fabrication of CNT-FED with diode structure is to be showed.

2.2.2 Gate Controlled Anode Current

Field emitters are made of CNTs that possess low turn-on voltages and thus operate at reasonable anode voltages in a diode mode. For a triode mode operation, the anode voltage has to be made as low as possible to avoid diode-type electron emission. At this anode voltage, an increase of gate voltage can ignite the electron emission from the nanotube emitters. In spite of some loss of electrons toward the gate electrode, the majority of emitted electrons can be attracted to the high-voltage anode.

Comparing the planar-gate and under-gate structure, we tried another method and expected that it might result in the same effects as the planar-gate and under-gate structure. First, the relative position of gate and CNT emitter tips were controlled by changing the thickness of the gate dielectric. We assumed that the gate under or upon the CNT emitter tips might be modulated by this way if the CNT height was fixed, as shown in Fig. 2-8.

Huh et al. synthesized vertically aligned CNT emitters on iron-deposited trenches by thermal CVD [2.21]. The depth of the trenches was about 1 um and the length of the CNTs approximated to 10 um. The triode structure was similar to our under-gate structure. Besides, they also showed the excellent gate controlled anode current. Although they didn't refer to the under-gate structure, we supposed it was like the under-gate structure which we had proposed.

The CNTs grown at low temperature might result in the fact that the length of the CNTs was always restricted by the physical limit. If we can control it, the triode structure of planar-gate and under-gate should be adjusted by the length of CNTs. In this thesis, we tried

to compare the two structures introduced above, and we anticipate that the under-gate structure exhibits desirable gate controlled anode current.

2.2.3 CNT-FED on Glass Substrate

In order to apply CNTs to field emission display, it is necessary to cost down by growing CNTs on glass substrate. For this reason, we used the glass substrate for CNT synthesis at low temperature of 500℃. The CNTs grown at low temperature in this thesis would be synthesized on glass substrate with the same parameters. Since this is the first time that we tested the process in our team, we fabricated the diode structure but not the triode structure due to the lack of mature techniques. In this thesis, a CNT-FED with complete diode structure is to be fabricated by thermal CVD at low temperature.

Chapter 3

Experimental Procedures

3.1 Introduction

Three structures were fabricated for the CNT-FED in this chapter. First, we used several metals as the catalysts for CNT synthesis and found the most fitting ones for CNT growth at low temperature. Then we fabricated triode structure on Si substrate and diode structure on glass substrate to prove the superiority of novel alloy catalysts in CNT-FED. According to the Tammann's rule, NiPd and FeC were employed as the catalysts for the first time in the present thesis in growing CNTs. Finally, the CNT emitters on glass substrate for field emission display were produced. The scheme of the whole experimental procedures was shown in Fig. 3-1.

3.2 Low Temperature Growth of CNTs

3.2.1 Forward Arrangement

A (100) n-type silicon wafer was prepared for the substrate. After the RCA clean and lithography processes, we defined three kinds of patterns (squares of 1000、100、10 um^2) for CNT field emission arrays. A 500Å Ti layer was deposited by dual E-gun evaporation (JAPAN ULVAC EBX-10C) as the buffer layer between the substrate and catalyst. Different catalyst layers were deposited sequentially and their relative parameters were shown in Table 3-1.

Among these catalysts, FeNi and NiPd were co-deposited in slow depositing rate and FeC was deposited with a sputtering target which contained 4.3% C and 99% purity by sputtering system (ENGLAND Ion Tech Microvac 450CB). After the deposition of the catalysts into the patterns as described above, the photoresist was lifted off in acetone solution. At last, the samples were already accomplished for CNT growth.

3.2.2 CNT Synthesis

The samples with different catalysts were transferred into a thermal CVD chamber (Fig. 3-2). First, the catalyst film must be pretreated to form nano-particles with H_2. It is more difficult for catalyst film to become particles without plasma treatment. Then, the hydrocarbon gas source was added to synthesize CNTs. In this instrument, there were two types of hydrocarbon gases: CH_4 and C_2H_4. Because of the differences of chemical reactivity, we applied C_2H_4 (more reactive) to synthesize CNTs in general. The whole experimental process was presented schematically in Fig. 3-3.

To synthesize CNTs, several experiments were proceeding. In experiment A, B, C, D, E, and F, we grew CNTs with different catalysts at 500~700 ℃ and there will be an exhaustive investigation in the following section of results and discussions. In experiment F, we compared different composition proportion of Ni and Pd. The process temperatures of experiments A, B, C, D, E and F were 700℃, 600℃, 500℃, 500℃, 500℃ and 500℃ for each. The experimental parameters of CNT synthesis were described as follows:

Experiment A、B、C:

The catalysts' nano-films were pretreated with 400 sccm H_2, and 500sccm N_2 for 5 minutes. Then 20 sccm C_2H_4 was added instead of CH_4 to grow CNTs with the same flow rate of H_2 and N_2 for 10 minutes.

Experiment D & F:

The catalysts' nano-films were pretreated with 400 sccm H_2 for 5 minutes. Then 20 sccm C_2H_4 was added to grow CNTs with the same flow rate of H_2 for 60 minutes.

Experiment E:

The catalysts' nano-films were pretreated with 400 sccm H_2 for 5 minutes. Then 20 sccm C_2H_4 was added to grow CNTs with the same flow rate of H_2 for 120 minutes.

Table 3-2 presented clearly the experimental process.

We had tried the same conditions for CNT growth at different temperatures, but the CNTs seemed to be synthesized with different conditions at high and low temperature respectively. For this reason, we designed distinct and suitable conditions for CNT growth at different temperatures. The conditions for CNT growth at low temperature were obtained from experimental experiences. They were special, however, unsuitable for CNT growth at high temperature (above 550 ℃).

3.3 Triode Structure on Si Substrate

3.3.1 Structure Fabrication

The fabrication procedures of the triode structure for CNT-FED were shown in Fig. 3-4. A (100) n-type silicon wafer was provided as the substrate. As shown in Fig. 3-4(a), a 5000 Å and a 10000 Å thermal SiO_2 layers were grown by wet oxidation furnace on different wafers respectively. Right after that, a 2000Å poly-Si layer was deposited on the SiO_2 by low pressure chemical vapor deposition (LPCVD) for the gate electrode, as shown in Fig. 3-4(b). The poly-Si was further doped with $POCl_3$ diffusion source at 950℃ for 30 minutes and then phosphorous was driven in at 950℃ for 30 minutes. Consequently, a poly-gate structure was

constructed. The sheet resistance of poly-Si was measured 40Ω/□ by 4-point probe. In photolithography processes, we isolated device by the first mask and defined different cathode areas by the second mask as described in section 3.2.1 (Fig. 3-4(c)).

The poly-Si and SiO_2 films in cathode region were dry etched by employing anisotropic mechanism by high density plasma reactive ion etching system (HDP-RIE) as illustrated in Fig. 3-4(d). The poly-Si and SiO_2 films were continuously etched in lateral direction by wet etching solution for 10 seconds and 3 minutes respectively (Fig. 3-4(e)). With the previously patterned photoresist layer as the shadow mask, a 500 Å Ti and a thin alloy (NiPd and FeC) layer were deposited directly on the patterned Si substrate by dual E-gun and sputtering system successively (Fig. 3-4(f)). Finally, the Ti and catalyst layers on photoresist were removed by the lift-off method as presented in Fig. 3-4(g), and transferred into the thermal CVD chamber for CNT growth immediately as displayed in Fig. 3-4(h).

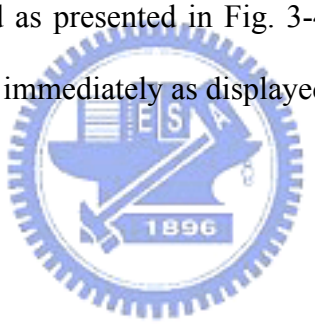

3.3.2 CNT Synthesis

Since the triode structure had been fabricated, we synthesized CNTs in thermal CVD chamber with NiPd and FeC as the catalysts at relatively low temperature. By means of the change of the gate dielectric's thickness, we tried to fabricate an under-gate structure and improve the field emission characteristics of the CNTs. In this section, thermal oxide with two different sorts of thickness was grown on Si wafer to build different gate structures. We assumed that the distance of gate to CNT emitters would result in different field emission properties. The experimental parameters were described as follows:

Experiment G & H:

The catalysts' nano-films were pretreated with 400 sccm H_2 for 5 minutes. Then 20 sccm C_2H_4 was added to grow CNTs with the same flow rate of H_2 for 120 minutes.

The relative parameters of thermal CVD process were presented in Table 3-3.

3.4 CNTs Grown on Glass Substrate

3.4.1 Sample Preparation

A glass substrate, PD200, was prepared for CNT synthesis. PD200 was produced by ASAHI GLASS COMPANY and given from TECONANO. Some characteristics of PD200 and soda-lime glass were shown in the Table 3-4. The PD200 was prepared as a rectangular of 2 cm x 3.4 cm for the conformable size in thermal CVD chamber. Before using PD200 as the substrate, we cleaned it in a 75% alcohol solution. The continuous process was shown completely in the Fig. 3-5. A 3000 Å Mo was firstly deposited as a cathode electrode by sputtering system (Fig. 3-5 (a)). Following that, a 500 Å Ti buffer layer was deposited on the Mo film by dual E-gun as shown in Fig. 3-5(b). By using a shadow mask with three kinds of circular patterns (radius: 100um、200um、400um), a 50 Å NiPd film as the catalyst metal was deposited on the Ti buffer layer in the patterns subsequently (Fig. 3-5 (c)). Finally, the shadow mask was removed and the diode structure on glass substrate was transferred to thermal CVD chamber for CNT growth as shown in Fig. 3-5(d).

3.4.2 CNT Synthesis

The sample of patterned catalyst film on glass substrate was loaded into the thermal CVD chamber for CNT growth. In order to avoid the melt of PD200 and contamination of the chamber, we set a Si wafer under the glass substrate. Then we synthesized CNTs as described in the following:

Experiment I:

The catalysts' nano-film was pretreated with 400 sccm H_2 for 5 minutes. Then 20 sccm C_2H_4 was added to grow CNTs with the same flow rate of H_2 for 120 minutes.

Table 3-5 showed the parameters of the growing process.

3.5 Analysis

Surface morphology and internal structure of CNTs synthesized in our experiments were characterized by a Hitachi S-4700I high-resolution field-emission scanning electron microscopy (SEM) and high-resolution transmission electron microscopy (HR-TEM) respectively. In addition, Raman spectra revealed the two peaks of CNTs (graphite and defect). The electric characteristics were measured by Keithley 237 (Fig. 3-6) in a 10^{-6} torr chamber. We also applied an ITO glass with phosphor coating on it as the anode to observe the luminescent image.

Chapter 4

Results and Discussion

4.1 Low Temperature Growth of CNTs

4.1.1 Temperature Dependence (Experiment A, B, C, D)

I. Pretreatment

It is generally believed that the formation of catalyst nanoparticles is necessary before CNT growth. In order to form these nanoparticles of catalyst, we proceeded a procedure before CNT growth─ pretreatment. The pretreatment method is to balance the surface energy (catalyst/gas), interface energy (catalyst/substrate), and interior energy (body free energy) of catalyst's nanofilm at designated temperature, and then to achieve the purpose of nanoparticles' formation. The nanoparticles can not only help the CNT growth have better quality but also control the size and morphology of CNTs [4.1]. Therefore, the formation of nanoparticles plays an important role in CNT synthesis for device application.

There is a crucial issue before investigating the mechanism of nanoparticles' formation─ melting point. According to the Lindemann's criterion, the melting point is not a constant, but a function of material's size [4.2]. In one word, the smaller the size is, the lower the melting point is (Fig. 2-1). In our experiments, we grew CNTs at low temperature, and the melting point is a very important parameter during synthesizing CNTs. First we concerned whether catalyst's nanofilm could be transformed into nanoparticles or not. In experiments A, B, C, we observed the variation of nanofilm after the pretreatment process by SEM images as shown in

Fig. 4-1, 4-2, and 4-3. A nanofilm pretreated at a higher temperature (700℃) was transformed into nanoparticles with non-uniform size. Via lowering the temperature, we found that the nanoparticles became more invariable in size. We thought that the formation of non-uniform nanoparticles after pretreatment at higher temperature may be due to the higher energy and moving rate of atoms. This may explain that why the atoms congregated in a larger size more probably within the same amount of time when a nanofilm was pretreated at a higher temperature.

Moreover, we could discover the formation of nanoparticles at low temperature of 500℃. The conventional model of melting point may be not suitable for nano-size material. We supposed that the transformation of nanoparticles at a temperature (500℃) lower than the melting point of catalyst (1400~1500℃) should be based on the Lindemann's criterion. Besides, the melting point of nanoparticles could be much lower if they existed in the CNTs [4.3]. Thus, we reached a conclusion that the nanoparticles of various catalysts should be well formed at a low temperature after pretreatment. We were certain that the formation of catalyst nanoparticles was not the key handicap for CNT growth at low temperature.

II. Growth of CNTs

There are two primary stages of CNT synthesis: nucleation of graphite and growth of CNTs. In thermal CVD, the carbon atoms come from the decomposition of hydrocarbon gas. Through heating the furnace and the activation of catalyst, carbon atoms are gradually discharged from the gas source and diffused to the surface of nanoparticles. The graphite layer is finally formed at the surface of nanoparticles after the procedures of dissolution of carbon atoms into nanoparticles, diffusion at the surface or in the body, and saturation. The procedure described above is called "nucleation", which has impacts on the subsequent process of CNT

growth.

In light of the concept of thermodynamics, carbon atoms obtain more energy at higher temperature. Consequently, CNTs grown at higher temperature usually construct better graphite structure. Recently, how to grow CNTs at low temperature has become a crucial issue. Since some physical conditions restrict CNT growth at low temperature, we must choose more proper catalysts for nucleation of graphite and growth of CNTs. In the present study, we utilized several common (Fe, Ni, FeNi) and novel (NiPd, FeC) catalysts for low temperature CNT growth. Figures 4-4, 4-5, and 4-6 show the SEM images after growth process at 700℃ (Experiment A), 600℃ (Experiment B), and 500℃ (Experiment C) respectively. We could easily grow aligned CNTs at 700℃ with Fe, FeNi, and FeC as the catalysts. By lowering temperature, we found the change of morphology and density of CNTs. They were characterized by curled wires and the density became much lower. From our experiences, CNTs grown with Ni or NiPd as the catalysts were always non-aligned in morphology no matter what the temperature was. And curled CNTs could be improved by controlling the growth time, the catalyst layer thickness or the power if using MPCVD or PECVD [4.4-4.5].

In Experiment C, the CNTs were grown at 500℃ with the same conditions as Experiment A and B. From the images shown in Fig. 4-6, we could observe that CNTs were not grown easily at 500℃ compared with the results in Experiment A and B because of the addition of N_2 and H_2. N_2 and H_2 could not only dilute the carbon source but also suppress the decomposition of hydrocarbon gas. For this reason, we removed N_2 and H_2 in growing CNTs at low temperature in Experiment D.

Owing to the slower reaction rate at low temperature [4.6], we prolonged the growing time and expected this might contribute to the growth of CNTs. We found that it was useless for CNT growth with Fe, Ni, and FeNi as the catalysts. As shown in Fig. 4-7, we noted that the length of CNTs grown with NiPd and FeC as the catalysts was especially long at low

temperature by removing the N_2 as well as H_2, and extending the growth time. Aligned CNTs were grown successfully by using FeC as the catalyst while particularly long and curled CNTs were grown by using NiPd as the catalyst. We assumed that there should be a main reason explaining this phenomenon: the Tammann's temperature of NiPd and FeC is lower than Fe, Ni, FeNi, and it results in the activity of their nanoparticles for carbon atoms diffusing at the surface and in the body. The Fe, Ni, and FeNi particles are easily poisoned because they are not active enough for carbon atoms diffusing in them. By the continuous decomposition of hydrocarbon gas, the carbon atoms were dissolving into the catalyst's nanoparticles consecutively. If the subsequent process can not be proceeded to handle these carbon atoms, the nanoparticles will become inactive and expire finally.

Novel catalysts like NiPd and FeC which we used in growing CNTs at low temperature are special and different from other common catalysts like Fe, Co, Ni, FeNi etc. As far as NiPd is concerned, it is a unique catalyst for CNT growth. We found that NiPd seemed unsuitable for CNT growth at high temperature as shown in Figures 4-4, 4-5. The CNTs looked like cotton (700℃) and spike (600℃). Such particular structure was not seen in any other papers. When the temperature was lowered to 500℃, CNTs became more straight and various in diameter (Fig. 4-7). We thought that NiPd was not favorable for CNT growth at high temperature due to its extremely low melting point and high activity. Moreover, the ultra large grain of NiPd caused the cotton shape at 700℃. For FeC, CNTs grown with it as the catalyst looked more aligned and thinner than those grown with other catalysts at low temperature (Fig. 4-7). It resulted in high aspect ratio of CNTs. Besides, we supposed that it might be tip-growth model by SEM images with bright dot at tip of CNTs.

At low temperature, the solubility and diffusion coefficient are low, and hence, graphite nucleation of nanotubes starts from smaller grains first [4.7]. This effect coupled with the fact that smaller crystallites are more active (have a higher surface/volume ratio) can explain the

temperature effect on the tube diameter. Precipitation of carbon at grain boundaries readily detaches the smaller grains from the catalyst islands, initiating nanotube growth. As deposition continues, the grains where precipitation has not taken place in a coherent way because of asymmetries in the shape or too large size, become catalytically inactive and are covered by carbon layers either graphitic or amorphous. This implied that NiPd was an extremely active catalyst, because the CNTs grown at low temperature showed various size in diameter. The NiPd nanoparticles of greater size also revealed higher activity in growing CNTs.

The microarea Raman scattering spectrums of CNTs in our Experiment A, B, and D are displayed in Figures 4-8, 4-9 and 4-10, respectively. All the spectra clearly showed two sharp peaks at approximately 1350 cm^{-1} (D band) and 1580 cm^{-1} (G band), representing typical characteristics of amorphous and graphite carbons [4.8]. As shown in Fig. 4-8, CNTs grown with Fe, FeNi, and FeC as the catalysts seemed to have well graphite structure. On the other hand, the Raman spectra of CNTs grown with Ni and NiPd as the catalysts showed the existence of a large quantity of carbonaceous impurities. Further, we discovered that the Raman spectrum became weaker and broader at D band peaks in Figures 4-9 and 4-10. It revealed more amorphous carbon produced at low temperature. As compared with SEM images, it confirmed that the well graphite structure and more aligned morphology of CNTs usually followed the higher intensity of G band.

The field emission characteristics were measured by Keithley 237 as represented in Figures 4-11, 4-12, and 4-13. The distance between anode and cathode was kept at 120 um. For conventional catalysts, the field emission current decayed rapidly at the same electric field when the growth temperature was lowered to 500℃. Oppositely, the field emission characteristics of CNTs grown with NiPd and FeC as the catalysts were better than those CNTs grown with other catalysts, especially at lower growth temperature. It should be due to

the highly active capability of NiPd and FeC nanoparticles during CNT growth at low temperature. Relative electric characteristics, including turn-on field (defined at the current density 10 uA/cm^2) and current density (obtained at the applied electric field 6 V/um), were shown in Table 4-1 and Table 4-2 distinctly.

We presumed that there was a great correlation between the morphology of CNTs and the field emission characteristics. However, it was not sure whether the field emission sites came from well graphite structure or disordered defects so far [4.9-4.10]. Previous studies indicated that the emission source may come from high aspect ratio CNTs or defects at the surface of CNTs. However, FeC and NiPd are superior in low temperature CNT growth, because the CNTs reveal excellent field emission characteristics, inclusive of high current density and low turn-on field. Such a superiority of CNTs grown at low temperature based on NiPd and FeC may be due to high field emission sites density and high aspect ratio, respectively. As indicated in Fig. 4-14, relatively clear luminescent images of CNTs with NiPd as the catalyst on the ITO and phosphor coating anode were observed at applied electric field (a) 4.2, (b) 4.6, (c) 5, (d) 5.4, (e) 5.8, and (f) 6.3 V/um, respectively. Recently, we have fabricated CNT emitters for field emission display successfully at low temperature by thermal CVD.

4.1.2 Growth Time Effect (Experiment E)

We have known that the growth time have great influence on the length of CNTs [4.11]. The phenomenon exists at high temperature, whereas the length of CNTs grown at low temperature is not directly proportional to growth time. On the contrary, CNTs grown at low temperature with extended growth time will cause accumulation of carbonaceous impurities. Then the field emission characteristics may be deteriorated seriously. Fig. 4-15 showed the SEM images of the CNTs' morphology with the prolonging of the growth time from 1hour

(Experiment D) to 2 hours (Experiment E). The CNTs grown with conventional catalysts were similar to those grown in 1 hour. It implied the fact that the conventional catalysts' nanoparticles lost activity finally, so prolonging the growth time was useless for CNT growth with conventional catalysts at low temperature.

The length of CNTs with FeC as the catalyst is a little longer than that of CNTs grown in 1 hour. By contrast, prolonging the growth time is beneficial for CNT growth with NiPd as the catalyst. As shown in Fig. 4-15, the length of the CNTs grown with NiPd as the catalyst in 2 hours was longer than that of CNTs grown in 1 hour. The TEM images of CNTs grown with NiPd and FeC as the catalysts were shown in Fig. 4-16. We could find that there were many defects existing on the surface (as marked in Fig. 4-16) of CNTs grown with NiPd as the catalyst, but the CNTs grown with FeC as the catalyst showed aligned morphology. We thought the emission sites of CNTs with NiPd and FeC as the catalysts were different. With the former catalyst, electrons were emitted by the defects on the surface of tubes, while with the latter, electron were emitted by the CNT tips. There were more defects existing at the surface of the longer CNTs with NiPd as the catalyst. It resulted in an extremely high current density (152.3 mA/cm^2) at the same applied electric field (6 V/um) as shown in Fig. 4-17. For FeC, the longer length was useless for the field emission characteristics because the quantity of tips was the same as that in a shorter growth time. It is considered that the nanoparticles of NiPd always maintain their optimum activity for carbon dissolution, diffusion, and CNT growth. Thus it can be seen that NiPd is indeed a superior catalyst in the field of CNTs grown at low temperature.

4.1.3 Eutectic Point Influence (Experiment F)

In order to demonstrate the Tammann's rule as described in chapter 2, we designed an

experiment with various alloy composition to derive the eutectic point influence on CNTs grown at low temperature. Carbon atoms started to diffuse and move at the surface as well as in the body of the catalysts' nanoparticles above the Tammann temperature, which is about 1/3 of the melting point. In this experiment (Experiment F), Ni and different composition of NiPd were compared in growing CNTs at 500℃. The catalysts were Ni, NiPd (Pd:21%), NiPd (Pd:60%), NiPd (Pd:84%), and NiPd (Pd:92%) respectively. According to the phase diagram of NiPd alloy, the lowest melting point occurs when the weight percentage of Pd is 60%. Therefore, NiPd (Pd:60%) has a lowest Tammann temperature theoretically. The SEM images of CNTs were shown in Fig. 4-18. It seemed that the CNTs grown with NiPd (Pd:60%), NiPd (Pd:84%), and NiPd (Pd:21%) as the catalysts were more aligned in morphology. The CNTs with NiPd (Pd:92%) as the catalyst were grown in difficulty at low temperature. Raman spectra were shown in Fig. 4-19, and broad D peaks in all samples resulted from many defects existing on the surface of CNTs. After measuring the electric characteristics by Keithley 237, we found that CNTs grown with NiPd (Pd:60%) as the catalyst exhibited the best electric properties with lower turn-on field and higher current density as shown in Fig. 4-20. We thought that the superior electric characteristics of NiPd (Pd:60%) might be due to the higher activity of the nanoparticles for CNT growth and more emission sites. Such a result conformed to the Tammann's rule, and it was valuable that we discovered an excellent catalyst for CNT-FED at relatively low temperature.

4.2 Triode Structure on Si Substrate (Experiment G, H)

In the current study, an under-gate type triode structure which consisting of the gate electrodes locating underneath the cathode electrodes has been investigated as one of triode-type CNT-FEDs, mainly for its simple structure. We produced two kinds of triode structure here, including planar-gate and under-gate structures. From our experiences, CNTs

grown with FeC as the catalyst were vertically aligned and they could be grown at low temperature. Without any short between gate and cathode, we needed aligned CNTs in the defined patterns. Besides, the length of CNTs grown on FeC layer was more easily controlled than that of CNTs grown on NiPd layer. Therefore, we chose FeC as the catalyst in the triode structures.

Figures 4-21 and 4-22 showed the SEM images of under-gate and planar-gate structures. We observed that the CNT tips were above and under the gate electrode respectively. The triode under-gate and planar gate structures were fabricated simply by modulating the thickness of dielectric layer. In short, triode-type FEAs are essential for practical FED applications in order to realize low voltage driving, high resolution and full gray-scale imaging [4.12]. Although the gate electrodes were placed underneath the cathode electrodes, electron emission from CNT emitters could be easily modulated by gate voltage. The emission current density measured on anode of the under-gate structure was higher than that of the planar-gate structure at the same applied voltage, which indicated that the under-gate structure not only controlled the electron emitted from the CNT tips but also suppressed the gate leakage current effectively. For the under-gate structure, the electrons were pulled out by the gate voltage and then emitted to anode without passing through the gate. For the planar-gate structure, electrons emitted to the closer gate more easily and resulted in a higher leakage current. However, electron beam emitted in the planar-gate structure was more convergent than that emitted in the under-gate structure. Limited by the deficiency of the Keithley 237 in triode electric analysis, we could not validate the analytic results of electric characteristics in this section.

4.3 CNTs Grown on Glass Substrate (Experiment I)

For practical application of CNT-FED, we utilized glass as the substrate for CNT growth. PD200 was used as the glass substrate in our experiment. The melting point of PD200 is 570 ℃, and thus we proceeded our experiments at 500℃ to avoid the melt of the glass. For this reason, we had to choose the most effective catalyst for low temperature growth of CNTs. As discovered by us, NiPd and FeC seem to be the optimum catalysts. Although growing CNTs at low temperature is the tendency in the application of CNT-FED, there are still few papers referring to the low temperature growth of CNTs on glass substrate by thermal CVD. Since Mo and Cr are usually applied as the cathode electrode in CNT-FED on glass substrate, we chose Mo as the cathode electrode material in our experiment and used NiPd and FeC as the catalysts to grow CNTs.

In Fig. 4-23, (a) and (b) showed the SEM images of CNTs grown with FeC and NiPd as the catalysts respectively on the glass substrate by thermal CVD. CNTs grown on glass substrate with FeC as the catalyst revealed more curled morphology than those grown on Si wafer. The morphology of CNTs grown on glass substrate was different from that of CNTs grown on Si substrate. The diameter size of CNTs was more uniform on glass substrate. This intrinsic quality of substrate resulted in different growing condition of CNTs and the CNTs showed various features in glass and Si substrate. By using NiPd as the catalyst, we grew uniform CNTs in a large area of glass and obtained fine electric properties. The filed emission characteristics with low turn-on field and high emission current density of CNTs synthesized with NiPd as the catalyst on glass substrate were shown in Fig. 4-24. In Fig. 4-25, (a) and (b) showed the image of CNT film by optical microscope and the luminescent image that corresponded with the electron emission from the CNTs was gained on the anode phosphor plate. The films under CNTs seemed to crack into many grains because of thermal stress. The luminescent image obtained on the anode with phosphor coating on it revealed non-uniformity a little. In order to solve this problem, we should concern the screen effect in a

large area CNT film [4.13]. However, it is gratified that we have fabricated CNT-FED on glass substrate by thermal CVD successfully, and we believe that the novel catalysts investigated in this thesis will improve the synthesis of CNT on flat-panel FED by thermal CVD.

Chapter 5

Conclusions and Future Prospects

5.1 Conclusions

Recently, the direct growth of CNTs on glass substrate by thermal CVD at low temperature has been researched for the fabrication of field emission displays. Owing to the higher throughput and better uniformity, thermal CVD is still the most attractive method for CNT growth. Although using soda lime glass substrate indeed costs down, the melting point of 570℃ restricts the processing temperature at which CNTs were synthesized by thermal CVD. Therefore, in the field of CNT-FED fabrication, how to grow uniform CNT films has been one of the most important issues. We started to research the growth mechanism of CNTs at low temperature and found that the conventional catalysts are not suitable for CNT growth at low temperature due to their higher melting point. In the study, two novel catalysts NiPd and FeC were investigated and used for CNT growth at relatively low temperature by thermal CVD. The field emission characteristics of CNT emitters grown with NiPd as the catalyst were superior than those of CNT emitters grown with other catalysts. The CNT emitters grown with NiPd as the catalyst at 500℃ for 2hrs exhibited a turn-on field 3.8 V/um and a current density as high as 152.3 mA/cm^2. Such excellent field emission properties of CNT-FED have not been proposed in any other papers before.

Moreover, we fabricated a triode structure with under-gate to improve the gate controlled anode current and to suppress the gate leakage current. In the under-gate structure, the electrons were pulled out by the gate voltage and then emitted to anode without passing

through the gate. The emission current density measured on anode of the under-gate structure was higher than that of the planar-gate structure at the same applied voltage.

For practical application of CNT-FED, we utilized glass as the substrate for CNT growth. By using NiPd as the catalyst, we have synthesized uniform CNTs on a large area of glass and obtained fine electric properties. The luminescent image corresponding with the electron emitting from the CNTs was gained on the anode phosphor plate. It is gratified that we have fabricated CNT-FED on glass substrate by thermal CVD successfully. We believe that the novel catalysts investigated in this thesis are helpful to the synthesis of CNTs for the application of flat-panel FED.

5.2 Future Prospects

For the synthesis of CNTs for field emission displays, the further research topics are presented as follows:

(1) Grow CNTs at low temperature (below 500℃) by thermal CVD

(2) Reduce density of CNTs to avoid screening effect

(3) Control alignment of CNTs to emit electron from tips

(4) Improve the uniformity and stability of CNT-FED

(5) Fabricate CNT-FED on glass substrate with triode structure

For the filed emission property investigation of CNTs:

(1) The long-term reliability should be researched.

(2) The field emission characteristics in different ambient including different gas, different catalyst and different pressure should be discussed.

For the CNT triode structures:

(1) The gate-to-emitter gap can be further reduced to lower the turn-on voltage.

(2) Optimum gate structure for the CNT triodes should be developed to reduce the gate leakage current.

(3) A prototype of CNT-FED must be demonstrated.